Transport Dynamics in Ordered Bilayer Assemblies of the *n*-Alkanes on Pt(111)

Adeana R. Bishop, Michael J. Hostetler, Gregory S. Girolami,* and Ralph G. Nuzzo*,†

Contribution from the Departments of Chemistry and Materials Science and Engineering and the Frederick Seitz Materials Research Laboratory, University of Illinois at Urbana-Champaign, Urbana, Illinois 61801

Received March 14, 1997

Abstract: The energetics of self-diffusion within ordered bilayer assemblies of linear hydrocarbons on Pt(111) (layer-to-layer) have been characterized using isothermal molecular beam-surface scattering in conjunction with temperature programmed desorption (TPD) and reflection-absorption infrared (RAIR) spectroscopies. The bilayers are prepared by layering a perdeuterated *n*-alkane on top of a perprotio *n*-alkane (or vice versa). The exchange of molecules between the two layers is weakly activated, less so than is either desorption of the multilayer from the substrate (the monolayer is more strongly bound) or the various phase transitions which lead to the loss of two-dimensional order in a corresponding densely-packed monolayer of the *n*-alkanes. The exchange process is further characterized by substantial size-asymmetry and isotope substitution effects which result in a preference for the selective retention of the longer and (for identical chain lengths) the protio hydrocarbon at the surface regardless of the initial deposition order. Layer-to-layer exchange occurs by a displacive mechanism which follows simple mass action principles: increasing the coverage of the post-absorbed species increases the extent of exchange. The difference in the activation energy for desorption (from the bilayer) and for exchange is ∼1.5 kcal/mol for both a C_8 and C_{10} perdeuterated *n*-alkane displacing an adsorbed (protio) chain of equal length. Thus, although the activation energy for self-diffusion increases with chain length, it is always less than the activation energy for sublimation by a constant amount. The implications of these results for energy dissipation mechanisms and relaxation dynamics in organic thin films are discussed and analogies to the properties of the so-called plastic-crystalline state are developed.

Introduction

Obtaining an improved understanding of such diverse phenomena as adhesion,[1] lubrication,[2,3] surface and interface induced organizations of molecular assemblies,[4,5] and heterogeneous catalysis[6] depends crucially on developing a clearer picture of the underlying dynamical properties of adsorbate-modified interfaces. Some important examples of relevant dynamic phenomena include adsorbate transport in boundary layers, adsorbate segregation, selective adsorption, lateral diffusion, and conformational relaxation and equilibration.

We present the results of a study which examines the self-diffusion of molecules between the two layers of a well-defined bilayer assembly. We show that hydrocarbon assemblies on Pt(111) serve as useful model phases for examining transport dynamics in thin organic films. The structure and thermodynamic properties of *monolayer* films of the *n*-alkanes on Pt(111) have been described in detail by us and others.[7,8] We build on this earlier work to develop an understanding of the phase behaviors seen in multilayer assemblies of the *n*-alkanes on this substrate, including those prepared from mixtures of adsorbates of varying chain length. We show that these films exhibit structures and behaviors similar to those observed in other thin-film and, so-called, two-dimensional mixtures.[9]

Monolayer thin films constructed from mixtures of two *different* adsorbates have been a focus of intense interest for many reasons not the least of which is the ease with which they lend themselves to the characterization of the thermodynamics of adsorbate−adsorbate and adsorbate−surface interactions.[10,11] The systems typically studied involve mixtures of monatomic gases (e.g., Xe, Ar) and/or small organic adsorbates (e.g., CH_4, etc.) in which the two components are physisorbed sequentially with total coverages varying from less than to a full monolayer; a weakly interacting substrate such as highly oriented pyrolytic graphite (HOPG) is most commonly employed in such studies.[12−14] For coverages of the mixed adsorbate pairs approaching one monolayer, several film growth habits have

* To whom correspondence should be addressed.
† Phone: (217) 244-0809. Fax: (217) 244-2278. E-mail: r-nuzzo@uiuc.edu.

(1) Tabor, D. *J. Coll. Interface. Sci.* **1977**, *58*, 2−13.
(2) Israelachvili, J. N. *Intermolecular and Surface Forces*; Academic Press: London, 1985.
(3) Reiter, G.; Demirel, A. L.; Granick, S. *Science* **1994**, *263*, 1741−1744.
(4) Nuzzo, R. G.; Korenic, E. M.; Dubois, L. H. *J. Chem. Phys.* **1990**, *93*, 767−773.
(5) Patrick, D. L.; Cee, V. J.; Beebe, T. P. Jr. *J. Phys. Chem.* **1996**, *100*, 8478−8481.
(6) Satterfield, C. H. *Heterogeneous Catalysis in Industrial Practice*; McGraw-Hill: Inc. New York, 1991.
(7) Firment, L. E.; Somorjai, G. A. *J. Chem. Phys.* **1978**, *69*, 3940−3952.
(8) Hostetler, M. J.; Manner, W. L.; Nuzzo, R. G.; Girolami, G. S. *J. Chem. Phys.* **1995**, *99*, 15269−15278.
(9) Hommeril, F.; Mutafschiev, B. *Phys. Rev. B* **1989**, *40*, 296−303.
(10) Rakotozafy, S.; Dupont-Pavlovsky, N.; Croset, B.; Duval, X. *Surf. Sci.* **1996**, *350*, 206−214.
(11) Asada, H.; Takechi, M.; Seiyama, H. *Surf. Sci.* **1996**, *346*, 294−299.
(12) Dupont-Pavlovsky, N.; Abdelmoula, M.; Rakotozafy, S.; Coulomb, J. P.; Croset, B.; Ressouche, E. *Surf. Sci.* **1994**, *317*, 388−396.
(13) Razafitianamaharavo, A.; Dupont-Pavlovsky, N.; Thomy, A. *J. Phys. France* **1990**, *51*, 91−102.
(14) Razafitianamaharavo, A.; Convert, P.; Coulomb, J. P.; Croset, B.; Dupont-Pavlovsky, N. *J. Phys. France* **1990**, *51*, 1961−1969.

S0002-7863(97)00835-4 CCC: $15.00 © 1998 American Chemical Society
Published on Web 03/21/1998

Scheme 1

Table 1.

postadsorbed	preadsorbed	substrate	temp (K)	ref
xenon	krypton	Pt(111)	40	63
krypton	methane	graphite	45−98	69
krypton	xenon	graphite	78−84	70
argon	xenon	graphite	11−132	64
nitrogen	carbon tetrachloride	graphite	77	17
argon	krypton	Pt(111)	30−36	15
krypton	cyclohexane	graphite	71−83	11−14
krypton	carbon tetrachloride	graphite	77−79	65, 66
methane	carbon tetrachloride	graphite	77	12
krypton	sulfur hexafluoride	graphite	70−80	67
xenon	dichloromethane	graphite	95−115	10
xenon	sulfur hexafluoride	graphite	80−112	68

been observed, the specifics of which depend strongly on the adsorbate pair studied. These growth habits are of two types: (a) the adsorbates phase separate into island domains (e.g., krypton and cyclohexane)[13] or (b) the adsorbates mix to form a two-dimensional solid solution (e.g., argon and krypton).[15] Depending on the exact nature of the lateral and substrate interactions, phase transitions which interconvert such phases are also possible.[16]

The phase behaviors seen at higher coverages (beyond a monolayer) are more complex. The most easily understood are those in which the second adsorbate interacts much more strongly with the substrate surface.[16] In this case, the latter adsorbate usually displaces the former from the surface; as the coverage is increased, three-dimensional islands of the first adsorbate are formed, and these eventually are lifted from the surface when the coverage of the second adsorbate is sufficient to saturate the first layer. This process is shown in Scheme 1. The displacement process need not be completely efficient and, as might be expected, the inverse adsorption order does not result in displacement. It is also possible, for systems showing coexistence of solid-solutions in the first layer, that an increase in the coverage of one of the components will also effect displacement of the partner by simple mass-action principles.[17] Specific examples are shown in Table 1 which suggest the diversity of the phase behaviors and structure/property correlations seen.

Clearly the most important factor governing whether mixing does or does not occur is the detailed balance established between the various adsorbate−adsorbate and adsorbate−substrate interactions.[9,16,18−20] One of the more intriguing examples of such an interplay is provided by the Kr/C_6H_{12} on graphite system where the driving force for the displacement is believed to be the energy released when the dense krypton monolayer is formed.[11] A paramount concern for the understanding of mixing kinetics is the underlying diffusion dynamics of the molecules and/or atoms involved. Such studies have been reported; notable examples of the latter include investigations of the diffusion of xenon atoms on Pt(111)[21] and Pt(11,11,9)[22] which suggested that the diffusion mechanism involves multiple site hopping. Recent studies utilizing TPD spectroscopies have provided evidence for a weakly activated diffusion of hydrocarbon radicals through alkane layers supported on Pt(111).[23]

Studies of the adsorption of *n*-alkane chains from solution onto graphite[24−27] offer further insights into the nature of the organizational and diffusion processes of *n*-alkanes at planar interfaces. For example, molecular dynamics simulations of a solution of a long-chain hydrocarbon in benzene confined between two graphite surfaces suggested that the alkane chains displaced the benzene molecules from the walls. The segregated chains adopt an organized habit in which their long axes align parallel to the plane of the graphite surface.[28] The confined chains are believed to show signs of a more long-ranged lateral ordering as well. Neutron diffraction studies of dotriacontane (n-$C_{32}D_{66}$) monolayers adsorbed on graphite from a perdeuterated *n*-heptane solution also have shown that the diffraction pattern one sees is different from that of a vapor deposited monolayer;[29] the authors suggest that a structural transformation is induced by the presence of a coadsorbed shorter chain hydrocarbon.

Experimental Method

Experiments were performed in ultrahigh vacuum using methods which have been described previously.[30] Only a brief overview is given here. Reflection-absorption infrared spectroscopy studies were performed in a stainless steel vacuum chamber equipped with turbomolecular, ion, and titanium sublimation pumps and having a base pressure of $<3.0 \times 10^{-10}$ Torr. The Pt(111) crystal was cleaned before each experiment by heating it in a 1.0×10^{-6} Torr atmosphere of dioxygen at 980 K for 5−8 min and subsequently annealing it at 1070 K. In most experiments, sample dosing was performed in a manner similar to the "preadsorbed layer" technique described in the literature.[31] The exposures were made from the background and were calibrated (for the ion gauge sensitivity) by RAIRS and TPD. To construct a sample, the clean Pt(111) crystal was cooled to a temperature lying between the monolayer and the multilayer desorption temperatures for the specific hydrocarbon being studied. After exposure to a flux equivalent to several tens of monolayers at this temperature, a well-ordered, full coverage monolayer was obtained. The dosing temperatures used for the various chain length hydrocarbons studied are hexane, 170 K; heptane, 185 K; octane, 190 K; nonane, 205 K; decane, 230 K. After dosing, the pressure was allowed to recover completely before the crystal was cooled to 110 K, at which point subsequent components could be dosed and the multilayer assembly formed. At this temperature, the partial pressure of the surface bound component is negligible, and the second component adsorbs only on the hydrocarbon precovered surface.

To effect transport of chains in the assembly, the temperature of the crystal was ramped quickly to a selected limiting value, equilibrated for several minutes, and cooled rapidly back to 110 K where the RAIRS spectrum was then taken. These spectra thus provide a snapshot of

(15) Zeppenfeld, P.; Becher, U.; Kern, K.; David, R.; Comsa, G. *Surf. Sci. Lett.* **1993**, *297*, L141−L147.
(16) Patrykiejew, A.; Sokolowski, S.; Zientarski, T.; Asada, H. *Surf. Sci.* **1994**, *314*, 129−143.
(17) Asada, H.; Doi, S.; Kawano, H. *Surf. Sci.* **1992**, *265*, L232−L238.
(18) Marti, C. C.; Croset, B. *Surf. Sci.* **1994**, *318*, 229−241.
(19) Mahale, N. K.; Cole, M. W. *Surf. Sci.* **1986**, *176*, 319−326.
(20) Mutaftschiev, B. *Phys. Rev. B* **1989**, *40*, 779−782.
(21) Meixner, D. L.; George, S. M. *J. Chem. Phys.* **1993**, *98*, 9115−9125.
(22) Sneh, O.; George, S. *J. Chem. Phys.* **1994**, *101*, 3287−3297.
(23) Tsai, Y.-L.; Koel, B. E. *J. Phys. Chem. B.* **1997**, *101*, 4781−4786.
(24) Watel, G.; Thibaudau, F.; Cousty, J. *Surf. Sci. Lett.* **1993**, *281*, L297−L302.
(25) Herwig, K. W.; Newton, J. C.; Taub, H. *Phys. Rev. B* **1994**, *50*, 15287−15297.
(26) Hansen, F. Y.; Taub, H. *J. Chem. Phys.* **1987**, *87*, 3232−3245.
(27) Thibaudau, F.; Watel, G.; Cousty, J. *Surf. Sci. Lett.* **1993**, *281*, L303−L307.
(28) Hentschke, R.; Winkler, R. G. *J. Chem. Phys.* **1993**, *99*, 5528−5534.
(29) Herwig, K. W.; Matthies, B.; Taub, H. *Phys. Rev. Lett.* **1995**, *75*, 3154−3157.
(30) Wiegand, B. C.; Lohokare, S. P.; Nuzzo, R. G. *J. Phys. Chem.* **1993**, *97*, 11553−11562.
(31) Singleton, J. H.; Halsey, G. D., Jr. *J. Chem. Phys.* **1954**, *58*, 330−335.

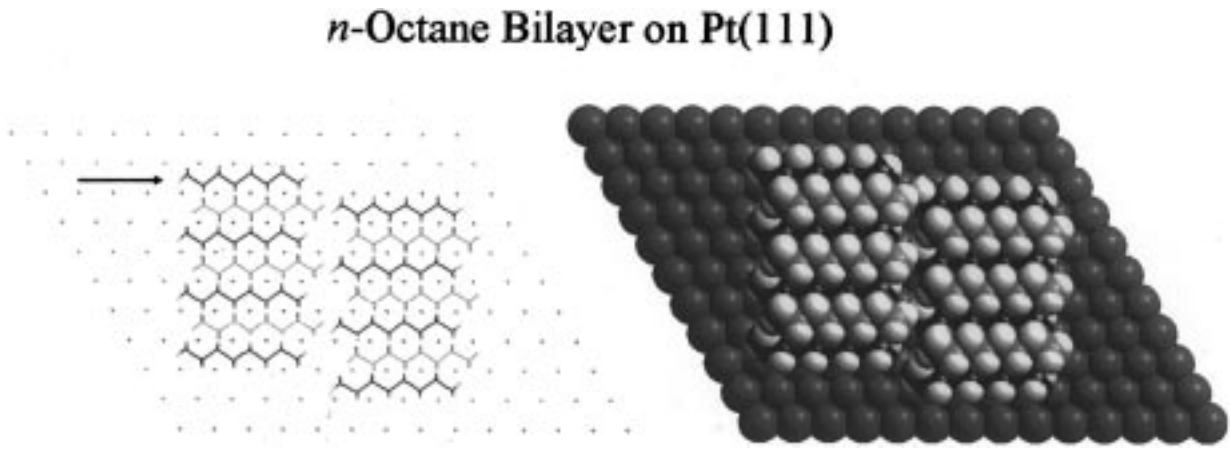

Figure 1. Proposed multilayer structure of *n*-octane on a Pt(111) surface. The unit cell dimensions deduced from LEED data are 12.7 Å × 4.80 Å within a single plane of molecules.[7]

the system at the equilibration temperature since controlled experiments revealed that few rearrangements of the system occur at 110 K.

To facilitate the differentiation of the two components in both infrared and desorption studies, a fully deuterated hydrocarbon was used to form either the preadsorbed or postadsorbed layers. This allowed the discrimination of the various methyl and methylene C−H (C−D) stretching modes. The significant perturbations of these modes, which result from direct metal contacts, enable the determination of the orientations and relative positions of the hydrocarbons within the layers on the platinum surface. Further, the desorption of each species could be independently monitored by TPD due to the difference in masses which obtain for the major cracking fragments. The specific ions followed were $m/e = 43$ for the perprotio hydrocarbon species and $m/e = 50$ for the perdeutero analogs.

The linear alkanes hexane (99+%), heptane (99%), octane (99+%), octane (d_{18}) (98+%), nonane (99%), and decane (99+%) were purchased from Aldrich, while decane (d_{22}) (99%) was purchased from Cambridge Isotopes.

Results

Normal alkanes, such as *n*-octane, adsorb on Pt(111) at low temperature to afford an overlayer in which all-trans chains are aligned along a specific high symmetry direction of the substrate (i.e., along the [1$\bar{1}$0] direction)[7,8] with their molecular plane aligned parallel to that of the surface. The structural scheme shown in Figure 1 illustrates one model of this structure (for an *n*-octane bilayer as a representative example) which is consistent with all the data presently available (primarily from RAIRS and LEED).[7,8] This scheme is likely an idealized depiction of the structure present at a high coverage of chains in the second layer. We show below (and describe in detail elsewhere) that the heat of absorption of chains bound in the second layer is only slightly greater than that of molecules residing in a third (or higher) layer. Chains in contact with the metal surface are much more strongly bound, however. For these reasons, the second layer should be populated by chains with some preference over the nucleation and growth of a third layer. The balance of the energetics appears to be such, though, that this need not occur with complete efficiency as the coverage in the bilayer approaches saturation.

The most salient structural points to note in the idealized model, though, are the chain spacing, alkane-layer contacts with the Pt surface, and interlayer registries of the chains. We discuss each briefly in turn.

First, the bilayer structural motif appears to closely mimic the habit found in the bulk triclinic crystal. The spacing shown results in a commensurate, high symmetry set of C−H···M contacts for the *n*-alkane chains (for all chain lengths) on Pt(111). The c-lattice constant of the bulk triclinic structure, however, is slightly shorter (see below) than that inferred from LEED data for the surface confined film.[32] Second, the exact structural nature of the C−H···M contacts still are not known precisely. Our data are consistent with bindings at either atop or bridged sites but other possibilities (e.g., 3-fold hollows) cannot be rigorously excluded. Finally, the multilayer organization is believed to stagger the chains layer-to-layer in the manner shown in the figure. This dense packing arrangement is similar to but slightly expanded relative to that found in the aforementioned bulk phases.

RAIRS Studies. Since Pt(111) is a metallic substrate, selection rules are imposed such that only those vibrational modes of the adsorbed layer with components of the transition moment oriented normal to the surface can be observed by RAIRS. An ordered array of hydrocarbons such as that described above would therefore give a RAIRS spectrum that differs significantly from that observed for an isotropic arrangement of the chains. This "dichroism" allows the orientation of the adsorbate to be deduced. The adsorption of the *n*-alkanes on Pt(111) introduces another perturbation to the spectra which is heavily exploited in this study to deduce precise details of the molecular organization. The C−H···M (and similarly the C−D···M) contacts induce significant perturbations of the optical functions relative to those of an unbound molecule. The direct contacts result in significant mode softening[8] with red shifts of more than 140 cm^{-1} being seen for the C−H stretches of those hydrogen atoms that are proximal to the surface. The stretching motions of the distal (nonmetal contacting C−H bonds) are also perturbed but to a lesser degree (∼16 cm^{-1}). We have previously described these effects and their application as a diagnostic probe of the order-order phase transitions which occur in the monolayers of *n*-alkanes on Pt(111).[8] Molecules present in the upper layer of a bilayer thin film do not exhibit these perturbations; the various C−H (and C−D) stretching vibrations appear in the regions normally associated with these modes and exhibit line shapes and peak frequencies similar to those seen for crystalline (bulk) samples of hydrocarbons.[8]

In the present study, we take advantage of the frequency shifts which accompany isotopic labeling to probe the exchange of hydrocarbons between the layers of a surface-bound bilayer. *These studies establish unambiguously that the self-diffusion of chains in these assemblies is weakly activated and character-*

(32) Mathisen, H.; Norman, N.; Pedersen, B. F. *Acta Chem. Scand.* **1967**, *21*, 127−135.

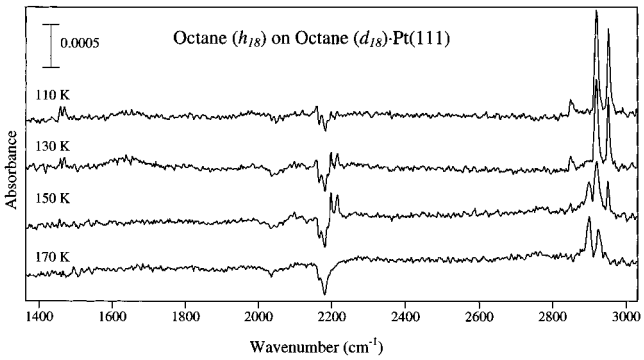

Figure 2. RAIR difference spectra of octane on octane (d_{18})·Pt(111) as a function of increasing annealing temperature. Features in the ∼2150−2250 cm^{-1} correspond to the C−D stretching modes of dC8, while features in the ∼2850−2960 region correspond to C−H stretching modes of C8. As is evidenced by the appearance and disappearance of modes, octane displaces some surface bound octane (d_{18}).

ized by a barrier which is less than that required to desorb chains from the multilayer.

Two variations of RAIRS are employed. The first uses a single-beam reference spectrum collected on the clean crystal prior to dosing. The spectra recorded in this way thus give absolute absorbance values. The second method is difference spectroscopy in which the value $-\log(R_2/R_1)$ is calculated for two single beam spectra, one collected after each adsorption step in the construction of an isotopically labeled *n*-alkane bilayer superlattice. In this manner, the (unperturbed) spectroscopic contributions of the first layer are self-normalized and, thus, not seen in the absorbance spectra. Perturbations to modes of the first layer (e.g., from "solvation" or conformational effects due to the presence of a second layer), however, are strongly evidenced in the difference spectra. Owing to the isotopic labeling scheme used, layer-to-layer diffusion results in the appearance of highly characteristic difference bands. Because of the significant frequency differences that exist, the stretching modes of molecules displaced from the metal surface appear as (new) positive absorbance features while those which of necessity are lost (because of mass balance) appear as negative intensity features. A set of positive intensity bands are also seen for molecules that have moved from the upper to the lower layer.

Octane with Octane (d_{18}). Figure 2 shows RAIR spectra obtained for an isotopically labeled *n*-octane superlattice. As shown by these data, increasing the annealing temperature increases the quantity of the surface bound component that is displaced by molecules in the second layer. The spectra shown in the figure were obtained at several different annealing temperatures (130, 150, and 170 K) for an equivalent of one monolayer of *n*-octane (C_8) adsorbed onto a Pt(111) surface precovered with a monolayer of *n*-octane(d_{18}) (dC_8). Features in the ∼2150−2250 cm^{-1} region correspond to the C−D stretching modes of dC_8, while features in the ∼2850−2955 cm^{-1} region correspond to the C−H stretching modes of C_8. Bands (or components) in the difference spectra with negative absorbances imply a reduction in the intensity relative to the background spectra, which here corresponds to the single beam spectrum of adsorbed dC_8. The negative intensity features seen at ∼2162 and 2179 cm^{-1} in the spectrum taken prior to annealing suggest that either a small amount of the dC_8 has been displaced from the surface at 110 K or, more likely, that the presence of the second octane layer causes small shifts in the stretching frequencies for the adsorbed dC_8 layer. The assignment of these features to specific modes is complicated by the fact that the various stretching modes of dC_8 are both overlapped and significantly perturbed by the C−D···M interactions.[8] The shifts which result are reasonably well understood for C−H vibrations but less so for the isotopically labeled hydrocarbons. We tentatively assign the negative intensity components to distal C−H stretches of the methylene and methyl groups of dC_8. The strong features seen in the C−H region for the as deposited sample at 110 K (2920 and 2953 cm^{-1}) correspond to the antisymmetric methylene, (d^-), and antisymmetric methyl out-of-plane (r^-_b) C−H stretching modes, respectively.[33] The methyl bending mode (weak) is seen at 1373 cm^{-1}. The very weak features seen at 1457 and 2849 cm^{-1} are believed to be due to a low concentration of orientational defect structures at the ambient surface of the multilayer.[34]

As the annealing temperature is increased, significant changes are seen in the spectra. These are most evident, for example, in the spectrum taken after annealing the sample at 150 K. Of significant note is the appearance of carbon−hydrogen stretching modes of C_8 molecules experiencing direct metal−surface contacts; the new bands appearing at 2899, 2925, and 2944 cm^{-1} are assignable to modes of surface bound C_8.[8] The 2899 cm^{-1} band is assigned to the perturbed C−H stretching motions of surface bound methylene segments of the C_8 adsorbate, while the two bands at 2925 and 2944 cm^{-1} originate in C−H stretching motions of the methyl group. These complex vibrational mode assignments are summarized in Table 2 and are discussed in detail elsewhere.[8,34] The appearance of the new C−H modes is directly correlated with the pronounced changes seen in the C−D region, the pattern of which reveals that dC_8 molecules have been displaced to the second layer. As noted above, these spectra strongly establish that the self-diffusion in the bilayer assembly is both displacive in character and less activated than the desorption of molecules from the weakly bound second layer.

As the temperature is increased further, the bilayer ultimately desorbs and the complex difference bands in C−D region are lost, being replaced instead by a "hole" due to the fraction of adsorbate lost during the exchange/desorption process. As a control, we carried out a series of annealing cycles similar to those shown in the figure on a C_8 monolayer (but without adsorbing a second layer); no desorption of material was seen by RAIRS, a result further confirmed by the TPD data presented below (which show that the monolayer only desorbs with a significant rate at temperatures above ∼250 K). We also repeated the layer-to-layer exchange experiments but on a sample which had been exposed first to several annealing cycles with C_8 in the bilayer before adsorbing the dC_8; identical results were obtained. This result strongly argues against the possibility that the exchange is dependent on the presence of vacancies in the initial surface bound monolayer. Finally we note that there is no measurable dependence of the behavior on the rate of the temperature ramp. Based on inferences developed below, we believe such sensitivities should exist but are modest for the range of ramp rates experimentally accessible with this instrument.

To complement the data shown in Figure 2, we inverted the deposition order used to construct the dC_8:C_8 bilayer. Similar layer-to-layer exchange behaviors of the chains were found when the sample was annealed (data not shown). As before, significant exchange occurs when the sample is annealed at 150 K. In this instance, the RAIR difference spectrum recorded after

(33) MacPhail, R. A.; Strauss, H. L.; Snyder, R. G.; Elliger, C. A. *J. Phys. Chem.* **1984**, *88*, 334−341.

(34) Bishop, A. R.; Nuzzo, R. G. Manuscript in preparation.

Table 2. Mode Assignments for *n*-Octane (h_{18}) and *n*-Octane (d_{18}) on Pt(111)[8,33]

	CH_3 δ(C−H)	CH_2 δ(C−H)	CH_2[a] ν(C−H)	CH_3[a] ν(C−H)	CH_2 ν(C−H)		CH_3 ν(C−H)	
					d^-	d^+	r^-	r^+
n-octane monolayer			2900	2928, 2944				
n-octane multilayer	1380	1457, 1469			2921	2850	2953	2874
n-octane (d_{18}) monolayer			2164	2179, 2206				
n-octane (d_{18}) multilayer					2198	(2093)	2216	(2125)

[a] The nature of vibrational modes for molecules interacting with the surface are sufficiently perturbed that the exact assignment of the symmetries of the modes remains somewhat ambiguious.[8]

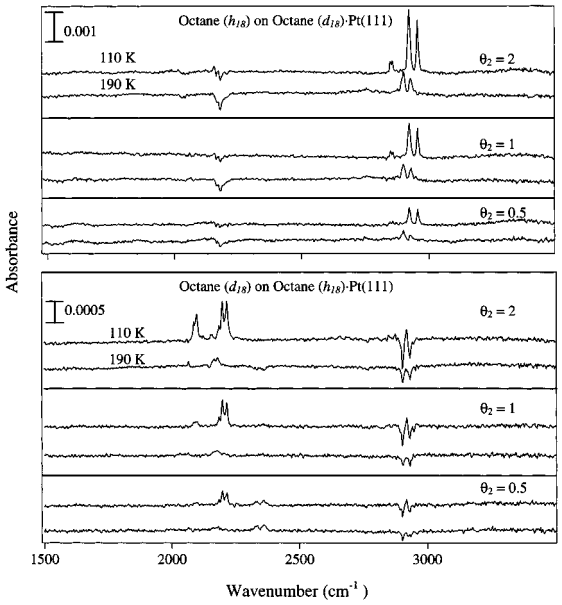

Figure 3. Top panel: Temperature dependent RAIR difference spectra of octane on octane (d_{18})·Pt(111) as a function of increasing octane coverage. Octane equivalents of two, one, and one-half monolayers are shown. With increasing octane coverage more surface bound octane (d_{18}) is displaced. Bottom panel: RAIR difference spectra of octane (d_{18}) on octane·Pt(111) as a function of increasing octane coverage. Octane (d_{18}) equivalents of two, one, and one-half monolayers are shown. With increasing octane (d_{18}) coverage more surface bound octane is displaced.

desorption of the weakly bound second layer at 170 K exhibits a pattern of bands in the C−H and C−D stretching regions, that is inverted relative to Figure 2. The intensities of the bands in the RAIR spectra suggest that the amount of C_8 displaced by dC_8 is less than that achieved by the inverse order of adsorption. This point is developed in detail later with the use of TPD data. We defer further discussion of this apparent isotope effect to that section.

The degree of exchange that occurs in the isotopically labeled multilayer varies with the mass coverage of the multilayer component. The spectra shown in Figure 3 correspond to a Pt(111) surface which had been dosed with a full monolayer of dC_8 (upper) or C_8 (lower) and then further dosed with approximately one-half, one, and two full monolayer coverages of the second adsorbate. The difference spectra taken at 110 K show the initial bound state. The systems were ramped to 190 K, thus desorbing the multilayer, and then cooled to 110 K where the second difference spectrum was taken. These latter spectra clearly show that the degree of exchange increases with the overlayer coverage. In addition there is a subtle isotope effect seen at all three coverages, one which can be inferred from a quantitative analysis of the data (see below). At all coverages, though, the difference spectra evidence a direct correlation between the intensity of the negative features in the C−D (or C−H) region and the intensity of positive features in the isotopically differentiated region. *This mass balance compellingly demonstrates that the self-diffusion occurring prior to the multilayer desorption is both displacive and mass action driven*. The nature of the underlying rate-phenomena involved in this "self-diffusion" process is developed in more detail below, and we defer their discussion to that point.

To investigate the kinetics of the exchange behavior further, corresponding isothermal scattering experiments were carried out. Exposure of a preformed monolayer to the second component was effected isothermally at a temperature above the multilayer desorption threshold using a finite flux dosed from the background. The data (given in the Supporting Information) show exchange behaviors similar to that seen in the temperature programmed studies (Figure 2). For example, the fraction of a monolayer of C_8 exchanging with dC_8 at a coverage of 2θ is substantial, corresponding to a coverage of $\sim 0.5\theta_{sat}$ of the first layer.

Heptane with Octane (d_{18}). To analyze the effects of the carbon chain length on displacive exchange, we examined by RAIRS various stratified pairings of *n*-heptane (C_7) and octane (d_{18}). These data are given in the Supporting Information. The spectra show that the structure of this mixed bilayer closely resembles that of the C_8:dC_8 system. For a bilayer of C_7 on dC_8, some exchange of the C−H and C−D segments takes place above 130 K. Further heating to 170 K completely reverses this degree of mixing and results in the desorption of the C_7. A bilayer of dC_8 on C_7, however, effects a nearly complete exchange using a similar temperature program. These observations suggest that the retention of the longer chain is strongly preferred. This conclusion also is supported by TPD data discussed below. These results suggest a size selection in which one methylene unit constitutes a significant bias in the equilibrium endpoint for exchange (we comment further on this point later in the paper).

Decane with Octane (d_{18}). The chain length preference noted above appears to be completely general, as further supported by the temperature dependence of RAIR spectra taken of two dC_8:C_{10} bilayer assemblies with inverted deposition orders (data given in Supporting Information). The size-asymmetry effects again are seen to strongly favor retention of the longer chain.

Quantitative Evaluation of the Energetics of Self-Diffusion in Isotopically Labeled Bilayers Using Temperature Programmed and Isothermal Desorption Methods. Two additional types of experiments based on mass spectral analysis were performed to quantitatively evaluate the energetics of the exchange processes occurring in the bilayer assemblies. The first, temperature programmed desorption experiments, allows a more precise quantitation of the degree of exchange and its sensitivity to mass action driving forces than is currently possible with RAIRS. This method is limited, though, by the fact that it only provides a snapshot of the equilibration as it exists at the desorption point of chains in the multilayer. The second method, a constant temperature desorption experiment, involves

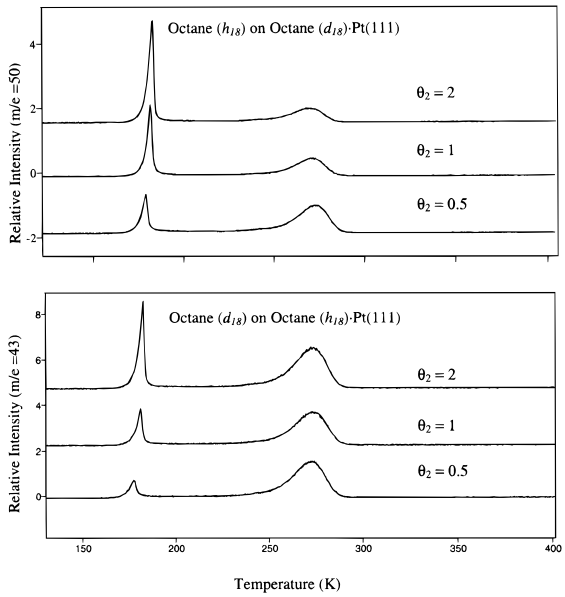

Figure 4. TPD spectra of isotopically labeled bilayers and multilayers showing desorption of the initially bound surface species. Upper panel: TPD for octane (d_{18}) on octane·Pt(111) showing the desorption of octane (*m/e* 43) as a function of two, one, and one-half equivalents coverages of octane (d_{18}). Lower panel: TPD for octane on octane-(d_{18})·Pt(111) showing the desorption of octane (d_{18}) (*m/e* 50) as a function of two, one, and one-half equivalents coverages of octane.

the use of an effusive molecular beam source to dynamically maintain a resident multilayer coverage at temperatures which are beyond those amenable to study by TPD.

TPD Studies. Temperature programmed desorption studies were performed by following masses which are specific indicators for the deuterio and protio isotopologs of a hydrocarbon pair (e.g., *m/e* = 50 for dC_8; *m/e* = 43 for C_8). For each pair studied, the monolayer and multilayer desorption temperatures are sufficiently different that two distinct peaks are observed. We can use the TPD data to determine the relative amounts of an isotopolog that desorb from either the monolayer or multilayer states. For C_8 on a dC_8 monolayer, the amount of dC_8 displaced from the surface increases as the amount of C_8 in the overlayer increases (Figure 4, upper panel). These data show, from top to bottom, the diffusional exchange which results when two, one, or one-half monolayers of C_8 are adsorbed onto the dC_8 precovered substrate. The lower temperature feature (centered at ~183 K) corresponds to the desorption of dC_8 from the multilayer (i.e., nonmetal-bound), whereas the higher temperature feature (~270 K) corresponds to the desorption of dC_8 from the Pt surface. A more detailed analysis of these desorption kinetics will be presented elsewhere.[34] The integrated intensities are very nearly constant in all three plots (as expected since only the amount of octane was varied). The increase in the intensity of the dC_8 multilayer desorption feature upon increasing the C_8 coverage firmly establishes the kinetic competence of *displacive exchange in the bilayer, a process which must have a lower activation energy than desorption from the low temperature multilayer state.* This confirms the inferences made on the basis of infrared data. Examination of TPD results for the reversed deposition order C_8:dC_8 system (Figure 4, lower panel) (using *m/e* = 43 as a specific cracking fragment of C_8) shows similar behavior albeit with one important quantitative difference.[35] Integrating the higher temperature TPD feature, dividing this value by the sum of the intensities of the monolayer and multilayer desorption features, and plotting these ratios as a function of the coverage of the second

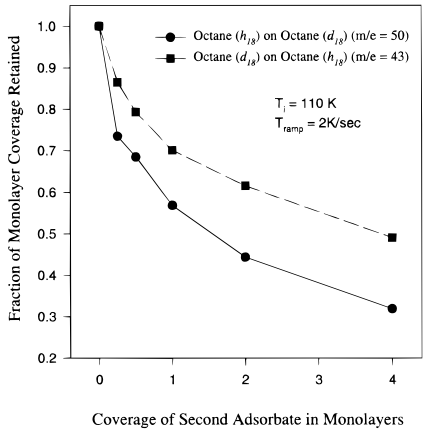

Figure 5. Comparison of coverage-dependent exchange measured by TPD for octane on octane(d_{18})·Pt(111) and octane(d_{18}) on octane·Pt(111) as deduced from self-normalized TPD peak areas.

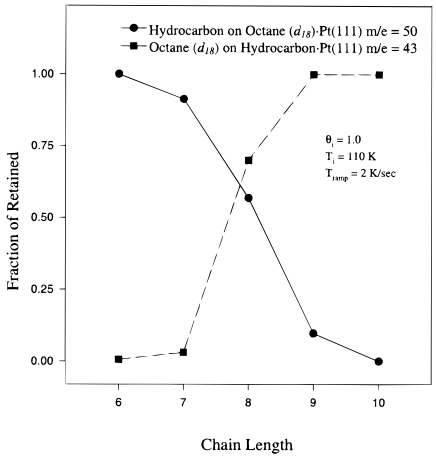

Figure 6. Comparison of bilayer exchange selectivity for carbon chain length asymmetries based on normalized TPD peak areas.

component in the overlayer yields the relationships shown in Figure 5 (these data were obtained from a more detailed set of experiments similar to those shown in Figure 4). At all coverages of the multilayer component, it is clear that dC_8 is more easily displaced from the first layer than is C_8. This result suggests that there is a significant isotope effect that favors retention of protio compounds in the lower (Pt-bound) layer by about a factor of 1.3−1.4. An isotope effect of this magnitude in a physisorbed system is unusually large. We believe this is a result of the underlying thermodynamics of the C−H(D)···metal contacts and comment further on this point later.

The chain length dependence of diffusional exchange was studied in a series of similar TPD studies but for a more restricted range of bilayer coverages (θ_2 = 1 monolayer equivalent). The sensitivity we find for the chain length asymmetry (C_6 to C_{10}) hydrocarbon is substantial (Figure 6). In these experiments we used dC_8 as a fixed reference and followed ions (*m/e* = 43 and 50) which are specific to the isotope content of the pair. As is clearly evident, there exists a near exclusive preference for the retention of the longer chain hydrocarbon at the surface regardless of hierarchical deposition order of the bilayer. This confirms the findings of the RAIRS experiments although we note that TPD is a simpler and more

(35) If we assume that the ionization fragmentation cross-sections are essentially temperature-independent (a reasonable assumption given the modest temperature range studied), the amount of C8 desorbing from either layer can be normalized, compared, and the functional form of the overlayer coverage dependence more directly determined.

Scheme 2

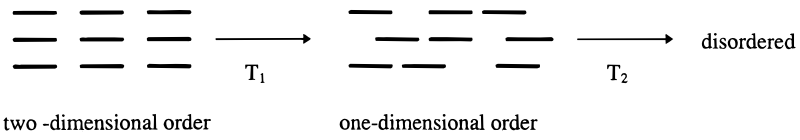

precise way of making such measurements (e.g., it clearly reveals the small amount of surface bound dC_8 that is displaced by C_7).

Isothermal Desorption Using Effusive Molecular Beam-Surface Scattering Methods. The second type of desorption experiment was performed at constant temperature. A well-ordered monolayer (of either C_8 or C_{10}) was first formed using the methods described previously, and the sample then was heated to a temperature in the range 170−240 K. The values were chosen so as to fall well within the "gap" defined by the multilayer and monolayer desorption peaks seen in TPD experiments (e.g., Figure 4). With the sample temperature held constant, a background pressure of the second component (either dC_8 or dC_{10}) was introduced using an effusive molecular beam source, and using a mass spectrometer, the desorption of the initially deposited protio-component was monitored. Representative data for the C_8:dC_8 system are given in Figure 7 and the Supporting Information. The initial rise in intensity results from the (nonideal) introduction of the second component via the opening of the last valve in source assembly; negligible desorption of the surface bound hydrocarbon occurs before the exposure to the second component. One qualitative trend can be seen in the data: as the temperature of the substrate is increased, the apparent decay time decreases. We present a quantitative analysis of this data in the Discussion section.

We also made a comparison of the waveforms measured at a common temperature for two different dC_8 fluxes (not shown). The backing pressure of the beam source was varied so as to yield effusive loads in the chamber of ∼6 and 3×10^{-8} Torr, respectively, in each experiment (i.e., a change in the beam flux of ca. a factor of 2). The shape of the desorption waveforms varied strongly with this change.

In the temperature regime in which these latter experiments were performed, the rate of desorption of any molecules in the multilayer should be fast and, therefore, the number present in the second layer should be both small and dependent on the sample temperature. RAIRS data (included as Supporting Information) shows this is in fact the case. Using the intensities which characterize the C−H vibrational modes of a C_8 bilayer and monolayer on Pt(111) at 110 K as a reference, the coverage maintained dynamically in the bilayer during the isothermal scattering experiment at 170 K is estimated to be less than ∼5−10% of that required to saturate the population of this layer. The coverages are even lower at the higher temperatures.

Discussion

The data presented above demonstrate the following points about ordered bilayer (and multilayer) assemblies of the *n*-alkanes on Pt(111). First, layer-to-layer exchange of molecules occurs in these phases. Second, this exchange—essentially the self-diffusion of the *n*-alkane molecule over a distance roughly of its own size—is weakly activated. More specifically, the barriers for this diffusional exchange must be less than the heats of sublimation of the *n*-alkanes examined since the data strongly argue that the displacement occurs both before and/or commensurate with the onset of the desorption of molecules from the multilayer. Third, the exchange process is characterized by a measurable isotope effect. As a typical example, the pairing of C_8 and dC_8 gave a value of $k_e(h)/k_e(d)$ of ∼1.4 with C_8 being more efficient at displacing dC_8 from the surface than is the inverse. Fourth, the exchange is displacive in nature: *surface-bound molecules must be promoted commensurately to the overlayer in order to be replaced.* Fifth, diffusional exchange is extremely sensitive to adsorbate structure: a size asymmetry of even one methylene group strongly biases the selection of which chain will be preferentially retained on the metal. We now comment in detail on these issues and provide a context to help frame the larger significance of these findings.

It is known from both diffraction and spectroscopic data that *n*-alkanes form commensurately ordered monolayers on Pt(111). Thermally activated phase transitions have also been observed for these structures, the nature of which is illustrated in Scheme 2.[8]

Using *n*-octane as an example, it has been found that a two-dimensionally ordered monolayer phase exists over a wide temperature range. Most interestingly, at ∼212 K (T_1) this layer exhibits a reversible order−order phase transition in which a 1-D ordered state of the molecules is obtained. In this latter state, the essentially all-trans conformations of the chains are maintained along with a collective alignment of the long axis (so called bond-orientational ordering). Long-ranged translational correlations are lost in this 1-D phase, however. At higher temperatures ($T_2 \sim 230$ K), the layer "melts" completely in that diffraction (although not RAIRS) suggests all order is lost in the monolayer.[8] Both phase transitions are believed to occur via vacancy generation due to the thermal population of gauche-conformer defects in the overlayer. The structures of the alkane multilayers on Pt(111) are less clearly understood, but it is evident that they too are ordered (with the chains adopting habits reminiscent of the monolayer phases). To our knowledge, data establishing the occurrence of phase transitions in these layers have not been reported. We do know, however, that the chains in the multilayer are more weakly bound than are those contacting the metal substrate. It is thus, perhaps, the most interesting result of this study that the diffusion of the hydrocarbon chains from layer-to-layer in *n*-alkane bilayer assemblies on Pt(111) is facile. Using *n*-octane again as a benchmark, we have demonstrated that the displacive equilibration of the chains in an isotopically-labeled bilayer superlattice occurs at temperatures as low as 130 K. This is ∼40 K less than the bilayer desorption temperature and 82 and 100 K less than the order−order (2D−1D) and order-disorder phase transition temperatures of the monolayer, respectively. The exchange (and thus layer-to-layer diffusion) is facile even in the ordered regions of the monolayer phase diagram. The LEED pattern of the layer present in the isothermal scattering experiment carried out at 170 K, for example, is one characteristic of the well-defined

$$\begin{bmatrix} 2 & 1 \\ \bar{1} & 4 \end{bmatrix}$$

overlayer (the 2-D ordered phase).[7] Such long-ranged order not withstanding, we find that the overlayer is still being dynamically "turned-over", since all the molecules are ex-

changed in minutes. The isothermal scattering experiments discussed below allow the energetics of this underlying self-diffusion process to be calculated precisely.

Analogies to the work reported here can be drawn from studies of lateral diffusion in lipid bilayers.[36−38] Lipids, although defined by complex phase diagrams, can exhibit significant fluidity at room temperature, much more so, for example, than would be found in the crystalline phases of hydrocarbons of similar molecular weight. The fluid phases of lipid bilayers can persist over a broad temperature range and exhibit lateral diffusion rates unmatched by solid linear hydrocarbons, except possibly at temperatures very near their melting points (above, for example, the so-called rotator-phase transition temperature).[39−41] Solute diffusion in lipid bilayers and linear hydrocarbons are also strongly differentiated in terms of their energetics.[42] The structural habits of bulk hydrocarbons are not an accurate approximation of those found in lipids, however. The center of the lipid bilayer, for example, has a more diffuse density profile of end groups than does a bulk hydrocarbon in an ordered phase, and these end groups are known to strongly affect the rates of diffusion of small molecule solutes.

Perhaps the best analogies to the present work are provided by so-called "plastic-crystalline" phases which have been characterized for a variety of organic compounds in the solid state. In these phases, the molecules exhibit significant orientational disorder due to the large amplitude of thermally activated librations.[43] Plastic crystals are most commonly associated with highly symmetric molecules which have weak, nondirectional interactions with their neighbors.[44] For example, plastic crystalline phases of methane, neopentane, cyclohexane, and benzene have been discussed extensively in the literature.[45−48] The analogy between the rotator phases[39−41] of the *n*-alkanes and a plastic crystal has also been noted.[44] A defining characteristic of the plastic crystalline state is the occurrence of atypically facile self-diffusion. With this in mind, we turn to a consideration of the quantitative aspects of the transport energetics measured in this study.

Kinetic Modeling of Isothermal Scattering Data. A simple model can be derived which defines all the steps necessary to effect a layer-to-layer exchange of the hydrocarbon chains. We assume that there is a background flux of A and one monolayer of B bound to the surface at $t = 0$. The elementary steps which need to be accounted for in the kinetic expressions are as follows (where the subscripts g indicates the gas phase, 2 refers to a nonmetal-bound component, and 1 refers to a metal-bound component):

(a) Reversible adsorption/desorption of molecules in the second layer.

$$A_g \underset{k_d}{\overset{k_{ad}}{\rightleftarrows}} A_2$$

(b) Displacive exchange of the A and B components between the second and first layers.

$$A_2 + B_1 \underset{k_e'}{\overset{k_e}{\rightleftarrows}} A_1 + B_2 \qquad (1)$$

(c) Irreversible desorption of the B component from the multilayer.

$$B_2 \overset{k_d}{\rightarrow} B_g$$

The total coverage of molecules in the surface bound layer is saturated in this temperature region, thus

$$[A_1] + [B_1] = C_{sat} \qquad (2)$$

Since the coverage in the multilayer is small (as shown by RAIRS), a steady state approximation can be made for the coverage of B_2.

$$-k_e'[A_1][B_2] + k_e[A_2][B_1] - k_d[B_2] = 0 \qquad (3)$$

Likewise, a steady state approximation can also be made for A_2 (assuming a Langmuirian form for the bilayer isotherm at the limit of low coverage):

$$k_e'[A_1][B_2] - k_e[A_2][B_1] - k_d[A_2] + k_{ads}P_A = 0 \qquad (4)$$

The rate of desorption for B is given by

$$R_{des} = k_d[B_2]$$

Since second-layer coverage of B is small, the B lost from the first layer must go irreversibly into the gas phase, thus

$$R_{des} = k_d[B_2] = -\frac{d[B_1]}{dt} \qquad (5)$$

By solving eq 3 for $[B_2]$, eq 4 for $[A_2]$, and eq 2 for $[A_1]$ and substituting the results into eq 5, we obtain after rearranging

$$d[B_1]\left(\frac{k_e'C_{sat} + k_d}{[B_1]} + k_e - k_e'\right) = -k_{ads}k_eP_A dt \qquad (6)$$

Which upon integrating from $B_1 = C_{sat}$ to B_1 and $t = 0$ to t, gives

$$(k_e'C_{sat} + k_d)\ln\frac{[B_1]}{C_{sat}} + (k_e - k_e')([B_1] - C_{sat}) = -k_{ads}k_eP_At \qquad (7)$$

The dominance of the first term in eq 7 results in an exponential form for the decay (while the second term is linear). Fits of the experimental decay curves given below show an exponential dependence, and it is thus reasonable to conclude that the second term is small relative to the first. Ignoring the second term and solving for $[B_1]$ gives

$$\ln\frac{[B_1]}{C_{sat}} = \left(\frac{-k_{ads}k_eP_A}{k_e'C_{sat} + k_d}\right)t \qquad (8)$$

The denominator of the right hand side contains two terms, the first of which describes the exchange between the layers and the second desorption from the bilayer. Note, the form of this

(36) Galle, J.; Volke, F. *Biophys. Chem.* **1995**, *54*, 109−117.
(37) Almeida, P. F. F.; Vaz, W. L. C.; Thompson, T. E. *Biochemistry* **1992**, *31*, 7198−7210.
(38) Bultmann, T.; Vaz, W. L. C.; Melo, E., C. C.; Sisk, R. B.; Thompson, T. E. *Biochemistry* **1991**, *30*, 5573−5579.
(39) Ungar, G. *J. Phys. Chem.* **1983**, *87*, 689−695.
(40) Ungar, G.; Masic, N. *J. Phys. Chem.* **1985**, *89*, 1036−1042.
(41) Barnes, J. D.; Fanconi, B. M. *J. Chem. Phys.* **1972**, *56*, 5190−5192.
(42) Bassolino-Klimas, D.; Alper, H. E.; Stouch, T. R. *Biochemistry* **1993**, *32*, 12624−12637.
(43) Timmermans, J. *J. Phys. Chem. Solids* **1961**, *18*, 1−8.
(44) Sherwood, J. N. *The Plastically Crystalline State*; John Wiley and Sons: New York, 1979.
(45) Harris, K. R. *Physica* **1978**, *94A*, 448−464.
(46) Stejskal, E. O.; Woessner, D. E.; Farrar, T. C.; Gutowsky, H. S. *J. Chem. Phys.* **1959**, *31*, 55−65.
(47) McKay, P.; Sherwood, J. N. *J. Chem. Soc., Faraday Trans. 1* **1975**, *71*, 2331−2339.
(48) Fox. R.; Sherwood, J. N. *Trans. Faraday Soc. Trans. 1* **1971**, *67*, 3364−3371.

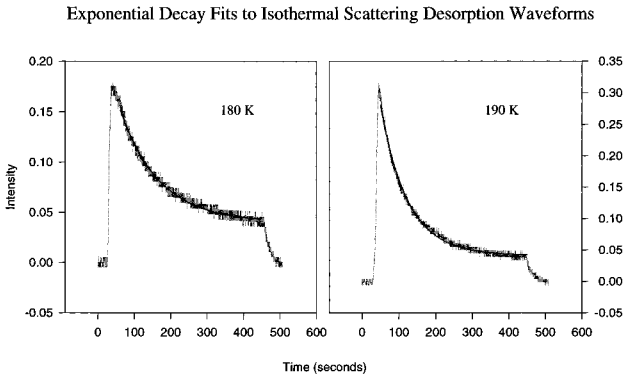

Figure 7. Representative experimental isothermal scattering waveforms for dC_8:C_8•Pt(111) and corresponding single exponential decay fits (solid dark line).

rate law is such that the decay will be exponential irrespective whether $k_e'C_{sat} > k_d$ or vice versa (see below). Thus the scattering waveform should be suitably modeled by a pseudo-first-order rate law (and hence as single exponential decay) if these assumptions are valid.

Figure 7 shows single exponential fits superimposed on two representative C_8:dC_8 scattering waveforms. The fits were made assuming a finite background level (due to desorption from the sample holder and walls of the vacuum chamber). As is evident on inspection, the fits are quite good and allow values of the apparent first-order rate constant (k_{app}) to be evaluated at each temperature.[49]

To extract the energetics from this information we need to examine the terms which define k_{app} more closely. The most important point of consideration is the kinetic competencies of the terms appearing in the denominator of eq 8. We ask which of the terms in the denominator is largest? If we assume that $k_d < k_e'C_{sat}$, then the model predicts that k_{app} should be essentially independent of the temperature of the surface; this prediction does not agree with the experimental data.[50] If we assume that $k_d > k_e'C_{sat}$, however, then a correct prediction of the temperature dependence of k_{app} results. With this we can rewrite k_{app} in Arrhenius form making the reasonable assumption that the sticking probability and, thus, the rate, k_{ads}, is weakly temperature dependent from 170 to 200 K.

$$k_{app} = (A_e \exp(-E_e/RT))\left(\frac{k_{ads}P_A}{A_d \exp(-E_d/RT)}\right) \quad (9)$$

Rearranging terms we obtain

$$k_{app} \approx k_{ads}P_A\left(\frac{A_e}{A_d}\right)\exp\left(\frac{E_d - E_e}{RT}\right) \quad (10)$$

Thus a plot of ln k' vs $1/T$ should yield a linear relationship whose slope is equal to the difference in the activation energies for desorption of the multilayer and exchange between the bilayers. Figure 8 shows plots of this analysis for scattering experiments carried out using C_8:dC_8 and C_{10}:dC_{10} pairs. The fits are excellent and support the suitability of the assumptions made in the kinetic model. Perhaps most intriguing is the fact that the differences in activation energies we measure ($E_d - E_e \sim 1.5$ kcal/mol) is independent of chain length. Using the values of the multilayer desorption energy reported elsewhere,[34] we can estimate the activation energies for the layer-to-layer diffusion. These values are 14.7 and 16.7 kcal/mol for C_8 and C_{10}, respectively (ignoring the modest contributions of the isotope effect, see below).

These values are reminiscent of those measured for the self-diffusion of molecules in the so-called plastic crystalline phases (more precisely, the orientationally-disordered solid phases) of organic molecules mentioned earlier.[44] A few specific examples serve to illustrate the trends seen. For methane, a self-diffusion activation energy of 4.78 kcal/mol has been reported.[44] Perhaps more relevant in the present context are the energetics of self-diffusion in the plastic crystalline state of cyclohexane, where a value of 21.77 kcal/mol is reported,[47] and (from radiotracer serial sectioning studies) eicosane ($C_{20}H_{42}$), for which activation energies of 81.5 and 38.5 kcal/mol have been reported for self-diffusion transverse and parallel to the basal plane of the crystal, respectively.[51]

The measured energetics of self-diffusion in the ordered *n*-alkane phase on Pt(111) are very unusual when compared with the energetics for sublimation. A metric of comparison suggested in the literature is the ratio of the activation energy of self-diffusion in bulk hydrocarbon phases to the heat of sublimation; reported values in the range of 1−2 are common.[44] For the thin-film phases studied here, these values (using the multilayer heat of sublimation as the reference) are all less than 1. This suggests that the density of the bilayer assembly is less than that of the structurally related triclinic phase. It is interesting to note that the systematic trends seen here agree with the conclusions reached by Brand et al. who have made complementary measurements in a related system.[52]

We now consider the more direct physical significance of the exchange energetics and the kinetic relationships from which they were obtained. It is most striking that very simple mass action kinetics are seen in this transport process. This implicitly establishes that the process does not involve complex dynamics such as might be expected, as an example, for the relaxation of a glassy phase. In this sense, then, the dynamics of the surface-bound hydrocarbons are quite typical, being intermediate between those of a crystalline solid and a liquid hydrocarbon. A more complete understanding of the energetics, though, requires that some model be invoked for the transition state being probed via the temperature dependencies of the various

(49) The data of the isothermal scattering experiment actually are recorded in the form of $I = f(t)$ where I, the intensity, is proportional to the instantaneous desorption rate at time t. This can be written for a first-order process as

$$I = c\frac{dA}{d} = -ck[A]_t$$

where c is a proportionality constant which contains the instrument response function. Using the integrated form of the rate law and substituting for $[A]_t$ we obtain

$$I = c\frac{dA}{dt} = -ckA_0 \exp(-kt)$$

Thus a fit of I as a function of t has k as a scalar. To account for the finite background and varying data range, we use the empirical relationship

$$y = C \exp(-k(t-t_0)) + y_0$$

as the functional form of the fit and iteratively evaluate values of C, k, and y_o until convergence.

(50) If this assumption did not hold, then one finds that the first-order rate constant is given by $(k_{ads}k_eP_A)/(k_e'C_{sat})$. For the isotopomeric pair used here it seems likely that $k_e \approx k_e'$ (since the isotope effect is modest in size). In this event, the temperature dependence seen in the scattering waveforms would arise only because of the temperature dependence of the sticking coefficient, but k_{ads} should be essentially independent of the surface temperature, and thus so should k_{app}.

(51) Narang, R. S.; Sherwood, J. N. *Mol. Cryst. Liq. Cryst.* **1980**, *59*, 167−174.

(52) Brand, J. L.; Arena, M. V.; Deckert, A. A.; George, S. M. *J. Chem. Phys.* **1990**, *92*, 5136−5143.

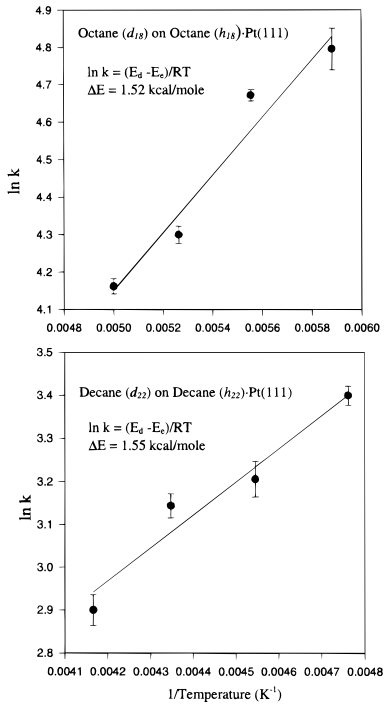

Figure 8. Temperature dependence of the self-diffusion energetics calculated from fits to isothermal scattering waveforms for C8:dC8. The slope of the line gives the difference in the energy of sublimation and the energy of exchange. For octane, this difference is 1.52 kcal/mol. Lower panel: Temperature dependence of self-diffusion energetics calculated from fits to isothermal scattering waveforms for c10:dC10. The slope of the linear fit gives the difference between the energies of sublimation and exchange. For decane, this difference is 1.55 kcal/mol.

rate constants. We know from diffraction data that the hydrocarbon adsorbates form dense monolayers on Pt(111). To be displaced from the metal, vacancies have to be generated. We believe this must occur via the thermal population of conformational (e.g., gauche) defects. Isomerization from trans to gauche conformers yields adsorbates with very different "footprints",[53,54] that is to say area projections, on the surface. The population of these conformational "defects" also provides a mechanism by which segments can be lifted from the surface in an incremental manner. In the present case, we see that the layer-to-layer exchange of the chains is displacive, that is to say that the substitution shows a clear mass-action dependence on both the adsorbate molecules which are displaced and those which displace them (rather than simply filling holes left by a rate-determining thermal desorption). This is also argued by the activation energy of the process (~1.5 kcal/mol less than the activation energy for desorption of a multilayer). If we assume a "quasi-local equilibrium", then substitution must occur progressively: for each segment of a first layer chain promoted to the overlayer, one in that layer moves to replace it. This suggests that dynamical motions at the chain ends are likely to be very important. It is also intriguing that the difference in the multilayer desorption and exchange activation energies that we measure in the isothermal desorption experiments (~1.5 kcal/mol) are small and chain length invariant (for C_8 and C_{10}). Perhaps coincidentally, it is a value which is also very close to the segmental interaction energy of the chain (i.e., the heat of interaction per carbon atom in the chain) in a bulk hydrocarbon

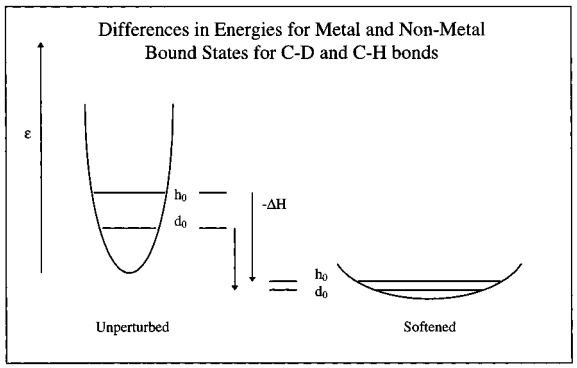

Figure 9. Schematic potential surfaces showing a qualitative rationalization for the retention preference of protio species in the surface bound layer. The potential well (approximated here as harmonic) corresponding to the surface bound state is softened relative to that of the unperturbed vibrational potential well. The energy change from the unbound to bound state is more exothermic for C−H than for C−D bonds due to the lower zero point energy for the C−D segments.

crystal[55] and the ground state energy difference between a trans and gauche conformer of an *n*-alkane in the gas phase.[56,57] It is therefore interesting to note that this barrier is essentially equal to the bias seen in the chain length asymmetry studies (i.e., an interaction energy difference of one methylene is sufficient to completely select the retention of one chain over another). A more precise interpretation beyond these potential correlations is currently lacking. Although our treatment of the kinetics is based on what is clearly a crude model, it does appear to capture the essence of the underlying transport processes and thermodynamics. It should be possible to define this mechanism more precisely, however, using molecular dynamics methods.

The Isotope Effect in Self-Diffusion. From the above discussion and a more comprehensive inspection of the literature, the basis of the isotope effect we have noted becomes obvious. It is our belief that it has to be reflective of the differences in the interaction energies of C−H and C−D bonds with the Pt(111) surface. To see how we arrive at his interpretation, it is useful to examine the thermodynamic aspects which follow most easily from the data. The data shown in Figure 5 demonstrate that exchange favors the retention of C−H contacts on the metal versus those of C−D segments. Using the ratio measured for a "stoichiometric" bilayer of dC_8 on C_8 after multilayer desorption, a value of $\theta_h \approx 0.7\ \theta_{sat}$ versus $\theta_d \approx 0.3\ \theta_{sat}$ is inferred for the preference of C−H over C−D contacts. If we write out a scheme for the equilibration of positions in an isotopically labeled superlattice

$$\theta_{1h} + \theta_{2d} \leftrightarrow \theta_{2h} + \theta_{1d} \tag{11}$$

it is possible to define an equilibrium constant as

$$K_e = \frac{(1 - \theta_{1h})^2}{(\theta_{1h})^2} \tag{12}$$

The experimentally measured value of $\theta_{1h} \approx 0.7$ ($K_e \approx 0.2$) reveals that this equilibrium position lies on the left side of the equation, a result inconsistent with ideal mixing (where $\theta_{1h} = 0.5$).

We note that this experimental result is one most reasonably directed by the underlying thermodynamics and not some aspect

(53) Hansen, F. Y.; Taub, H. *Phys. Rev. Lett.* **1986**, *69*, 652−655.
(54) Hansen, F. Y.; Newton, J. C.; Taub. H. *J. Chem. Phys.* **1993**, *98*, 4128−4141.
(55) Hoffman, J. D. *J. Chem. Phys.* **1952**, *20*, 541−549.
(56) Wiberg, K. B.; Murcko, M. A. *J. Am. Chem. Soc.* **1988**, *110*, 8029−8038.
(57) Mirkin, N. G.; Krimm, S. *J. Phys. Chem.* **1993**, *97*, 13887−13895.

of the kinetics. It is known, for example, that there exists an isotope effect for diffusion in bulk hydrocarbon phases, the magnitude of which is easily estimated for a variety of diffusion mechanisms. These effects are described by the relation[44]

$$\left(\frac{D_h}{D_d} - 1\right) = f\left[\left(\frac{m_d}{m_h}\right)^{1/2} - 1\right]$$

where D_i is the diffusion coefficient for the specific isotopomer, m_i is the corresponding mass, and f is a symmetry factor related to the crystal type and diffusion mechanism. For diffusion occurring via thermally activated vacancy generation in (as a specific example) a monoclinic crystal, f is less than 1: a value in the range 0.6−0.8 encompasses values appropriate to a range of crystal types. The net result is that the isotopic bias in the bulk diffusion rates of dC_8 and C_8 is small: as an estimate $D_h/D_d \approx 1.05$. This ratio directly reflects the isotope effect on the activation energies of vacancy generation. Since the displacive exchange examined here likely depends on vacancy generation occurring in the layer immediately adjacent to the metal (since it is most strongly bound there), a kinetic model predicts that C_8 should be more easily displaced than dC_8. This is opposite to the observed order.

Other isotope related features we have considered include (a) the difference in molecular size due to differences in C−H and C−D bond lengths[58,59] (that for C−H is greater by ∼0.002 Å); and (b) the difference in polarizability of C−H and C−D bonds[60] (generally greater, albeit slightly, for C−H). As before, these factors also are unable to explain an isotope effect of the magnitude seen here. The differences in polarizability would lead to an enrichment of dC_8 at the vacuum interface, much as occurs in isotopic polymer blends,[61] but this effect by itself is far too weak (for chains of this length) to account for the measured bias. The factors responsible for the isotope-dependent polarizabilities, though, point to the more fundamental contribution of interest here, namely the variation in the adsorbate vibrational contribution to the mixing potential due to anharmonicity and the zero point energy differences. The metal contacts lead to mode-softening and it is this interaction which clearly demonstrates the largest sensitivity to isotopic substitution. How this occurs can be qualitatively illustrated with the simple energy diagram shown in Figure 9. The softened C−H and C−D modes occur at lower frequencies than do the unperturbed fundamentals. As is suggested by the figure, this must lead to a larger energy change for the perturbed C−H bonds than for the C−D bonds due to the zero point energy differences. This qualitative picture, while instructive, is overly simplistic and not sufficiently detailed to allow a straightforward calculation of the difference in the energetics of C−H···M and C−D···M bonds. We note, however, that a difference in the segmental interaction energy (i.e., normalized to the chain length) of ∼0.1 kcal/mol (C−H > C−D) is sufficient to account for the effect measured experimentally. Shapley et al.[62−70] has in fact reported an isotope effect in the rotational equilibration of a series of progressively deuterated methyl groups in the multinuclear complex, $HOs_3(CO)_{10}CH_3$. He concluded that the rotomer with an C−H···Os interaction was more stable than the rotomer with a C−D···Os interaction by 0.13 kcal/mol. This value is remarkably similar to that inferred here from a qualitative analysis of the magnitude of K_e.

We will report a more detailed quantitative evaluation of this issue at a later time.

Acknowledgment. We gratefully acknowledge the support of the National Science Foundation (CHE-96-26871) and the Department of Energy (DEFG02-91-ER45439) through the University of Illinois Seitz Materials Research Laboratory.

JA970835I

(58) Kuchitsu, K.; Bartell, L. S. *J. Chem. Phys.* **1961**, *36*, 2470−2481.
(59) Bartell, L. S.; Kuchitsu, K.; DeNeui, R. J. *J. Chem. Phys.* **1961**, *35*, 1211−1218.
(60) Kaila, R.; Dixit, L.; Gupta, P. L. *Acta Physica Acad. Sci. Hung.* **1977**, *42*, 237−244.
(61) Jones, R. A.; Kramer, E. J.; Rafailovich, M. H.; Sokolov, J.; Schwartz, S. A. *Phys. Rev. Lett.* **1989**, *62*, 280−283.
(62) Calvert, R. B.; Shapley, J. R. *J. Am. Chem. Soc.* **1978**, *100*, 7726−7727.
(63) Zeppenfeld, P.; Kern, K.; David, R.; Becher, U.; Comsa, G. *Surf. Sci. Lett.* **1993**, *285*, L461−L467.
(64) Bohr, J.; Nielsen, M.; Als-Nielsen, J.; Kjaer, K.; McTague, J. P. *Surf. Sci.* **1983**, *125*, 181−187.
(65) Abdelmoula, M.; Ceva, T.; Croset, B.; Dupont-Pavlovsky, N. *Surf. Sci.* **1992**, *272*, 167−171.
(66) Asada, H.; Doi, S.; Kawano, H. *Surf. Sci.* **1992**, *273*, L403−L408.
(67) Bouchdoug, M.; Menaucourt, J.; Thomy, A. *J. Phys. France* **1986**, *47*, 1797−1804.
(68) Menaucourt, J.; Bockel, C. *J. Phys. France* **1990**, *51*, 1987−2003.
(69) Hamdi Alaoui, M. A.; Coulomb, J. P.; Dupont-Pavlovsky, N.; Mirebeau, I.; Mutaftschiev, B. *Surf. Sci. Lett.* **1993**, *295*, L1031−L1036.
(70) Regnier, J.; Bockel, C.; Dupont-Pavlovsky, N. *Surf. Sci. Lett.* **1981**, *112*, L770−L774.